EPILEPSY

Antisense oligonucleotides increase *Scn1a* expression and reduce seizures and SUDEP incidence in a mouse model of Dravet syndrome

Zhou Han[1], Chunling Chen[2], Anne Christiansen[1], Sophina Ji[1], Qian Lin[1], Charles Anumonwo[2], Chante Liu[2], Steven C. Leiser[3], Meena[1], Isabel Aznarez[1], Gene Liau[1], Lori L. Isom[2]*

Dravet syndrome (DS) is an intractable developmental and epileptic encephalopathy caused largely by de novo variants in the *SCN1A* gene, resulting in haploinsufficiency of the voltage-gated sodium channel α subunit $Na_V1.1$. Here, we used Targeted Augmentation of Nuclear Gene Output (TANGO) technology, which modulates naturally occurring, nonproductive splicing events to increase target gene and protein expression and ameliorate disease phenotype in a mouse model. We identified antisense oligonucleotides (ASOs) that specifically increase the expression of productive *Scn1a* transcript in human cell lines, as well as in mouse brain. We show that a single intracerebroventricular dose of a lead ASO at postnatal day 2 or 14 reduced the incidence of electrographic seizures and sudden unexpected death in epilepsy (SUDEP) in the F1:129S-*Scn1a*$^{+/-}$ × C57BL/6J mouse model of DS. Increased expression of productive *Scn1a* transcript and $Na_V1.1$ protein was confirmed in brains of treated mice. Our results suggest that TANGO may provide a unique, gene-specific approach for the treatment of DS.

INTRODUCTION

Dravet syndrome (DS; EIEE6, OMIM 607208) is a devastating form of developmental and epileptic encephalopathy. In greater than 80% of cases, DS is caused by de novo variants in *SCN1A*, encoding the voltage-gated sodium channel (VGSC) α subunit $Na_V1.1$, resulting in haploinsufficiency (*1*). DS is characterized by multiple pharmacoresistant seizure types, cognitive regression, ataxia, and increased mortality (*2*, *3*). Patients with DS have severe epilepsy, intellectual disability, developmental delays, movement and balance issues, language and speech disturbances, growth defects, sleep abnormalities, chronic infections, disruptions of the autonomic nervous system, and mood disorders (*4*). Although all patients with epilepsy are at risk for sudden unexpected death in epilepsy (SUDEP), patients with DS may have the highest risk, up to 20% (*5*). The mean age of SUDEP in patients with DS is 4.6 years (*6*). The prevalence of DS in the U.S. population has been estimated to be as high as 1:15,700 or a population of about 20,000 individuals (*7*). Although recently developed small-molecule anticonvulsant therapies, including stiripentol, Epidiolex, and fenfluramine (*8*–*10*), can provide partial seizure management in DS, there remains a substantial, unmet need for approaches to directly target brain *SCN1A* haploinsufficiency, the root cause of the disease.

Targeted Augmentation of Nuclear Gene Output (TANGO) technology, which uses antisense oligonucleotides (ASOs), has been developed to specifically increase protein expression (*11*). TANGO targets naturally occurring, nonproductive alternative splicing events to specifically reduce nonproductive mRNA and increase productive mRNA and protein of the target gene (*11*). Because TANGO can up-regulate the wild-type (WT) allele and thus compensate for the mutant allele in the context of autosomal dominant haploinsufficiency, this approach may provide a unique opportunity to develop therapeutics to treat this class of diseases, including DS.

Here, we used the TANGO approach to target a nonproductive alternative splicing event in *SCN1A* that results in nonsense-mediated decay (NMD) of the transcript. We targeted this NMD-inducing, or nonproductive, exon region with multiple ASOs and identified candidates that specifically decrease inclusion of this exon and increase the expression of productive *SCN1A* mRNA in cultured human cells. Intracerebroventricular (ICV) administration of a lead ASO in WT mouse brain increased the expression of productive *Scn1a* mRNA and $Na_V1.1$ protein. A single ICV dose of ASO at postnatal day 2 (P2) prevented SUDEP in 97% of DS mice up to 90 days after injection. Video monitoring of 19 DS mice injected with ASO at P2 showed a single tonic-clonic seizure followed by SUDEP in only 1 animal, with no behavioral seizures in the other 18. Electroencephalogram (EEG) recording of DS mice injected with ASO at P2 showed a reduction in seizure frequency with a prolongation in latency to first seizure. Together, our work provides preclinical rationale for developing this precision medicine approach to treat patients with DS.

RESULTS

Alternative splicing of *SCN1A* pre-mRNA that results in NMD is conserved in multiple species and in a patient with DS

NMD is a mechanism used by eukaryotic cells to degrade mRNA transcripts that contain premature termination codons (*12*). Naturally occurring, nonproductive alternative splicing events coupled to NMD are found in many genes and can be targeted via TANGO technology to increase gene expression (*11*). Bioinformatic analysis of human brain samples revealed an exon inclusion event in the *SCN1A* gene that leads to a frameshift and the introduction of a premature termination codon (*11*). Figure 1A shows a schematic representation and validation of this nonproductive splicing event by reverse transcription polymerase chain reaction (RT-PCR) of human cells treated with or without the translation inhibitor cycloheximide

[1]Stoke Therapeutics Inc., Bedford, MA 01730, USA. [2]Department of Pharmacology, University of Michigan, Ann Arbor, MI 48109, USA. [3]PsychoGenics Inc., Paramus, NJ 07652, USA.
*Corresponding author. Email: lisom@umich.edu

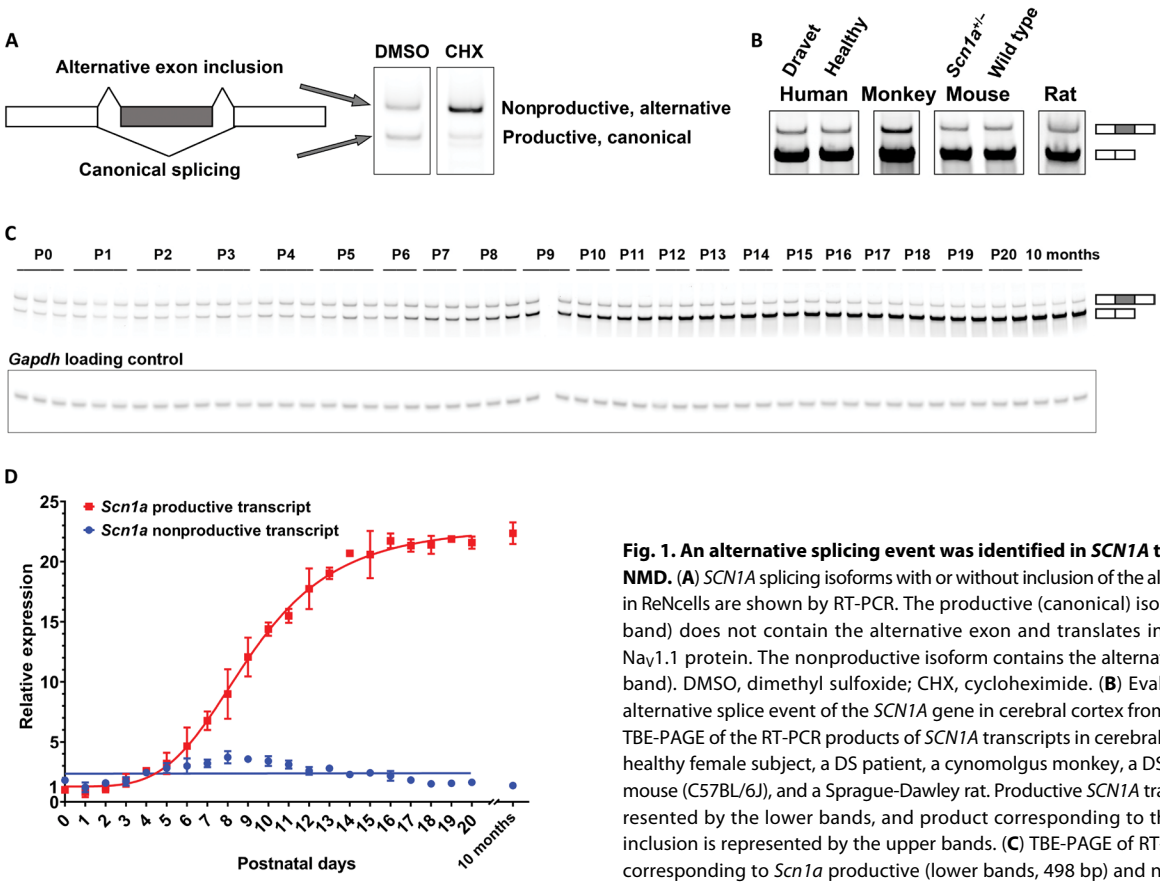

Fig. 1. An alternative splicing event was identified in *SCN1A* that results in NMD. (**A**) *SCN1A* splicing isoforms with or without inclusion of the alternative exon in ReNcells are shown by RT-PCR. The productive (canonical) isoform (bottom band) does not contain the alternative exon and translates into functional $Na_V1.1$ protein. The nonproductive isoform contains the alternative exon (top band). DMSO, dimethyl sulfoxide; CHX, cycloheximide. (**B**) Evaluation of the alternative splice event of the *SCN1A* gene in cerebral cortex from four species. TBE-PAGE of the RT-PCR products of *SCN1A* transcripts in cerebral cortex from a healthy female subject, a DS patient, a cynomolgus monkey, a DS mouse, a WT mouse (C57BL/6J), and a Sprague-Dawley rat. Productive *SCN1A* transcript is represented by the lower bands, and product corresponding to the NMD-exon inclusion is represented by the upper bands. (**C**) TBE-PAGE of RT-PCR products corresponding to *Scn1a* productive (lower bands, 498 bp) and nonproductive transcript (upper bands, 562 bp) amplified from total RNA extracted from C57BL/6J mouse brains from P0 to P20 and at 10 months. Mouse *Gapdh* was used as a loading control. (**D**) Expression of *Scn1a* productive and nonproductive transcript in postnatal mouse brains, calculated with optical densities of PCR products shown in (C). Expression of *Scn1a* transcripts was first normalized to endogenous *Gapdh* and then to the *Scn1a* productive transcript at P0. Data are presented as mean ± SD ($n = 2$ or 3 samples from individual animals for each data point). Expression of *Scn1a* productive transcript was fit to a four-parameter nonlinear curve. Expression of *Scn1a* nonproductive transcript was best fit to a linear curve.

(CHX). Basic Local Alignment Search Tool searches of the National Center for Biotechnology database identified highly conserved homologs of this *SCN1A* NMD-inducing exon in multiple species, and the results were verified by RT-PCR (Fig. 1B). Moreover, the presence of the NMD-inducing exon inclusion event is retained in brain tissues from a DS patient (Fig. 1B), suggesting that expression of the NMD-exon inclusion event is unchanged between healthy individuals and patients with DS.

The NMD-inducing transcript pool of *Scn1a* is maintained to adulthood in mice but is proportionally higher early in development

DS symptoms manifest during early postnatal development in humans and in mice (*4*, *13*). We performed RT-PCR analysis to measure the inclusion of the NMD-inducing exon and productive *Scn1a* mRNA in coronal brain sections from P0 to P20 and 10-month-old WT C57BL/6J mice (Fig. 1C). Densitometric measurement of the RT-PCR products showed that the NMD-inducing exon containing transcript (upper band) is largely unchanged during development, whereas the productive mRNA (lower band) increases (Fig. 1D). Productive *Scn1a* transcript expression (Fig. 1D) begins to increase markedly around P7 to P8. These results suggested that it may be possible to increase total productive transcript expression by converting NMD-exon containing transcripts to productive transcripts and that the impact of this manipulation would be the greatest during early postnatal brain development.

ASO administration increases *SCN1A* expression in cultured cells

We designed a series of ASOs that bind to human *SCN1A* exon 20N and the surrounding intronic sequences. All ASOs used in the initial screening were based on 2′-methoxy-ethyl modification of the oligonucleotide with a phosphorothioate backbone, known for its stability and low cytotoxicity (*14*). ASOs were screened in human neural progenitor cells by free uptake, followed by analysis of *SCN1A* productive and exon 20N–containing nonproductive transcripts with RT-PCR and quantitative PCR (qPCR). We identified a number of ASOs that decreased the NMD-inducing exon inclusion and increased productive transcript expression (Fig. 2, A to C). The most active ASO (ASO-22, indicated by the red arrow in Fig. 2, A to C) was selected for further evaluation.

Dose-response relationships for ASO-22 were determined in human neural progenitor cells using free uptake or nucleofection delivery methods. The EC_{50} (median effective concentration) values were 3 μM, determined by free uptake, and 514 nM, determined by nucleofection (Fig. 2D). We also investigated the specificity of ASO-22

by measuring its effect on the expression of four highly homologous VGSC α subunit genes in treated cells. No changes in the expression of *SCN2A*, *SCN3A*, *SCN8A*, or *SCN9A* were observed in ReNcells after 20, 8, or 3 μM ASO treatment via free uptake (Fig. 2E). A nontargeting ASO control (NT) had no effect on the expression of either transcript isoform but was active on its target (Fig. 2E and fig. S1). These results indicate that ASO-22 potently and specifically increases productive *SCN1A* mRNA in human neural progenitor cells.

Administration of ASO-22 results in dose-dependent, long-lasting, and specific increase in productive *Scn1a* mRNA and $Na_V1.1$ expression in mouse brain

To determine whether ASO-22 administration can up-regulate productive mRNA and protein in a dose-dependent manner in vivo, P2 WT C57BL/6J mice were dosed with a single ICV injection of ASO-22 at 0.3, 1, 3, 5, 10, 20, or 30 μg and euthanized 5 days after treatment (Fig. 3A). Brain tissues were collected and analyzed for changes in expression of nonproductive and productive *Scn1a* transcripts, respectively, as well as $Na_V1.1$ protein. Inclusion of the NMD exon in *Scn1a* transcript decreased with increasing ASO dose (Fig. 3B). We also observed a dose-dependent increase in productive *Scn1a* expression using probe-based qPCR (Fig. 3C) and RT-PCR (fig. S2), with a ~6-fold increase in expression detected in the 10-μg dose group, and no further increase was observed at 20 and 30 μg. Last, expression of $Na_V1.1$ protein increased in a similar dose-dependent manner (Fig. 3D and fig. S3). A nontargeting ASO control (NT) had no effect on the expression of *Scn1a* transcript (0.9 fold ± 0.1, $p > 0.05$) or $Na_V1.1$ (16.8% of adult expression ± 0.9%, $p > 0.05$) but was active on its target (fig. S4). The expression of eight closely related VGSC α subunit genes plus Nax (*Scn7a*) was unaffected in the brains of mice that had received the ASO (Fig. 3E).

To determine the durability of the ASO-22 effect in brain, P2 WT mice ICV-injected with 10 μg of ASO-22 were examined for brain expression of *Scn1a* productive transcript expression at varying time points after injection (Fig. 3F). Increased expression of productive *Scn1a* transcript was observed for up to 30 days after injection (Fig. 3G and fig. S5). $Na_V1.1$ protein expression also increased and was maintained during the 30-day observation period compared to phosphate-buffered saline (PBS) injection controls (Fig. 3H and fig. S6).

ASO administration increases $Na_V1.1$ protein expression and reduces the incidence of seizures and SUDEP in DS mice

We tested the effects of ASO-22 in the *Scn1a*^{tm1Kea} (F1:129S-*Scn1a*$^{+/-}$ × C57BL/6J) mouse model of DS, in which exon 1 of *Scn1a* is deleted, resulting in haploinsufficiency (*13*). These mice typically have a ~50% rate of premature mortality due to SUDEP (*13*), although this rate is known to vary between different laboratories and mouse facilities. We tested the efficacy of ASO-22 on SUDEP incidence in DS mice. PBS or a single 20-μg dose of ASO-22 was ICV-injected to DS mice and their WT littermates at P2, and survival monitoring began at P17 (Fig. 4A). Cohorts of injected mice from each group were euthanized at 7 or 14 weeks after injection for analysis of ASO exposure, target engagement, and $Na_V1.1$ expression in the brain (Fig. 4A). Cohorts euthanized at 7 weeks were not included in the 90-day survival analysis. Kaplan-Meier analysis showed that ASO-22 injection resulted in survival of 97% of DS mice (1 of 34 died) up to 90 days (Fig. 4B). In contrast, 23% of littermate DS mice treated with PBS survived during this time period (48 of 62 died) ($P < 0.0001$) (Fig. 4B). Thus, ASO treatment resulted in greater than fourfold improvement in survival of the DS mice. ASO exposure, target engagement, and $Na_V1.1$ expression were compared between ASO- and PBS-treated DS mouse brains (Fig. 4, C to H). We found that brain tissues had robust exposure to the ASO (~13 μg/g, 7 weeks after injection and ~8 μg/g, 14 weeks after injection). Expression of $Na_V1.1$ protein increased in ASO-treated DS mouse brains to amounts indistinguishable from WT brains (Fig. 4, G and H). The expression of *Scn1a* productive transcript and $Na_V1.1$ protein in the brains of ASO-injected WT animals also increased over PBS-treated WT animals; however, we observed no obvious impact of ASO treatment on the survival of WT animals over the 90-day period (Fig. 4B).

We next asked whether ASO-22 administration at P14, closer to the time of seizure onset (*15*) and just before the plateau of productive *Scn1a* transcript expression in WT mouse brain (Fig. 1D), could prolong survival in our DS mouse model. For this experiment, we increased the ASO dose relative to the increase in brain weight at the time of injection (Fig. 5A). Figure 5B shows that a single 60-μg ICV injection of ASO-22 at P14 resulted in 85% survival (45 of 53, $P < 0.005$) of ASO-injected DS mice compared to 64% (47 of 74) of PBS-injected DS mice, with no detectable effects on survival of the 40 ASO-treated *Scn1a*$^{+/+}$ WT mice, up to 90 days. Thus, ASO administration at P14 resulted in a 1.3-fold improvement in survival of DS mice. Liquid chromatography–mass spectrometry (LC-MS) analyses detected ASO in the brains of the P14 injected animals out to 90 days (Fig. 5, C and D). ASO treatment beginning at P14 also resulted in increased *Scn1a* mRNA and $Na_V1.1$ protein in DS brain at the P90 time point as well as in WT brain at both time points (Fig. 5, E to H). There was no significant impact of ASO-22 on expression of $Na_V1.1$ protein after injection at P14 when the data were evaluated at P35 (Fig. 5G).

Previous work using extensive video-electroencephalographic monitoring of F1:129S-*Scn1a*$^{+/-}$ × C57BL/6J DS mice demonstrated a 1:1 correlation between behavioral tonic-clonic and electrographic seizures, validating visual assessment of generalized tonic-clonic seizures in this model (*15*, *16*). We injected cohorts of DS mice with either a 20-μg ICV dose of ASO-22 at P2 (19 mice), a 60-μg ICV dose of ASO-22 at P14 (11 mice), or PBS at P14 (4 mice) and monitored them for behavioral tonic-clonic seizures by video recording (with infrared cameras to record behavior during the dark cycle) from P17 to P35. We observed a single tonic-clonic seizure followed by SUDEP in 2 of the 4 PBS-injected mice, but in only 1 of the 19 P2-injected mice and in only 2 of 11 P14-injected mice within the observation period. Movies S1 and S2 show terminal seizure events for one P14 ASO-injected DS mouse and one PBS-injected DS mouse, respectively. No generalized seizures were observed in any of the remaining 18 P2 or 9 P14 ASO-injected mice within the observation period. Thus, these data suggest that ASO administration at P2 and P14 likely reduces the incidence but not the severity of generalized tonic-clonic seizures in DS mice.

To monitor electrographic seizures, a separate cohort of DS mice ($n = 21$ per group) and WT littermates ($n = 11$ to 12 per group) received a 20-μg ICV injection of ASO-22 or PBS at P2, underwent surgery to install EEG headmounts at P20, and then were continuously monitored by EEG from P22 to P46 (Fig. 6A). DS mice that received ASO-22 had significantly fewer seizures during the recording period compared to their PBS-treated littermates ($P < 0.05$; Fig. 6B). In addition, administration of ASO-22 significantly prolonged latency to first seizure in DS mice during the recording period

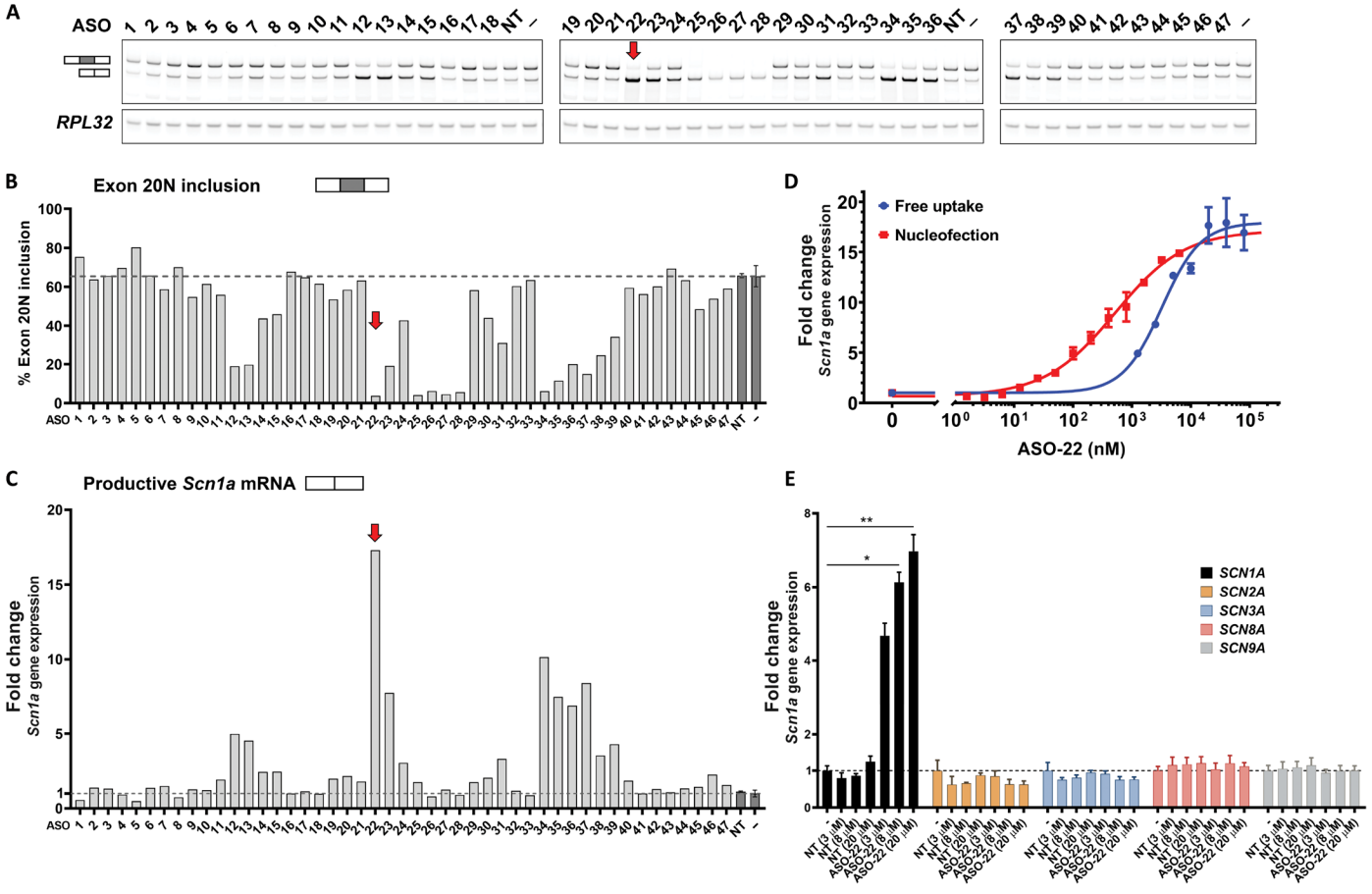

Fig. 2. Selected ASOs suppress the NMD splicing event and increase the expression of productive *SCN1A* mRNA in ReNcells. (**A**) ASO screen in ReNcells. TBE-PAGE of RT-PCR products corresponding to *SCN1A* productive (lower bands, 549 bp) and nonproductive mRNA containing exon 20N (upper bands, 613 bp) in ReNcells after gymnotic (free) uptake of ASO. A total of 47 ASOs were screened at 20 μM. A nontargeting ASO (NT) and no ASO control (–) were included. *RPL32* was used as loading control. Red arrow: Selected ASO (ASO-22) that resulted in the largest increase in productive *SCN1A* mRNA expression. (**B**) Percentage of exon 20N inclusion in *SCN1A* transcript, as quantified from the RT-PCR products shown in (A). PCR products were quantified by densitometry and plotted as percentage of the exon 20N–containing mRNA over total (exon 20N–containing and productive mRNA). Red arrows denote the selected ASO-22 ($n = 1$ for each ASO treatment group; $n = 2$ for NT; $n = 13$ for no ASO control). (**C**) Expression of *SCN1A* productive mRNA in ASO-treated ReNcells determined by SYBR green qPCR. Expression of *SCN1A* productive mRNA was first normalized to endogenous *RPL32* and then to no ASO control (–). qPCR results were presented as mean ± SD for each treatment. Red arrows denote the selected ASO-22 ($n = 1$ for each ASO treatment; $n = 2$ for NT; $n = 10$ for no ASO control). (**D**) Dose-response relationship of ASO-22 in ReNcells with free uptake and nucleofection. Expression of *SCN1A* was normalized to endogenous *RPL32* and then to no ASO control. qPCR results were presented as mean ± SD ($n = 2$ for both treatments). Expression of *Scn1a* productive transcript was fit to four-parameter nonlinear curves. (**E**) Effect of selected ASOs on expression of homologous VGSC α subunit genes in ReNcells. Expression of *SCN2A*, *SCN3A*, *SCN8A*, and *SCN9A* in ReNcells was measured by probe-based qPCR, following gymnotic uptake of 3, 8, or 20 μM ASO-22 or a nontarget ASO control (NT). *SCN* mRNA expression was first normalized to endogenous *Gapdh* and then to no ASO control (–). qPCR results were presented as mean ± SD for each analysis ($n = 4$ for each ASO treatment; $n = 8$ for no ASO control). For comparison of means, Kruskal-Wallis test followed by Dunn's multiple comparisons test was performed. *$P < 0.05$ and **$P < 0.01$. A list of qPCR assays used here was provided in Materials and Methods.

($P < 0.05$; Fig. 6C). EEG of ASO-22–treated DS mice is normally similar to EEG recorded from WT mice (Fig. 6D). However, when a seizure was observed in ASO-22–treated DS mice, the morphology of the seizure appeared similar with respect to amplitude, spike content and duration to those observed in PBS-treated DS mice (Fig. 6D). Thus, although the incidence of behavioral tonic-clonic seizures was markedly reduced in ASO-treated DS mice, electrographic seizures could still be detected. There were no differences in the number of seizure-free mice (48% PBS versus 76% ASO-22; $P > 0.05$) or in the number of mice having two or more seizures (38% PBS versus 14% ASO-22; $P > 0.05$) over the assessment period after ASO-22 administration (fig. S7). WT mice injected with ASO-22 at P2 ($n = 12$) did not exhibit abnormal EEG activity during the recording period (Fig. 6D).

DISCUSSION

DS is a complex, intractable developmental and epileptic encephalopathy. Some currently available anticonvulsant drugs provide limited prophylactic seizure relief for some patients with DS; however, all patients develop multiple, life-altering disease presentations over time and suffer serious side effects of polypharmacy (*17*). It is clear that a precision medicine approach, which directly targets *SCN1A* haploinsufficiency, is required to tackle this devastating disease.

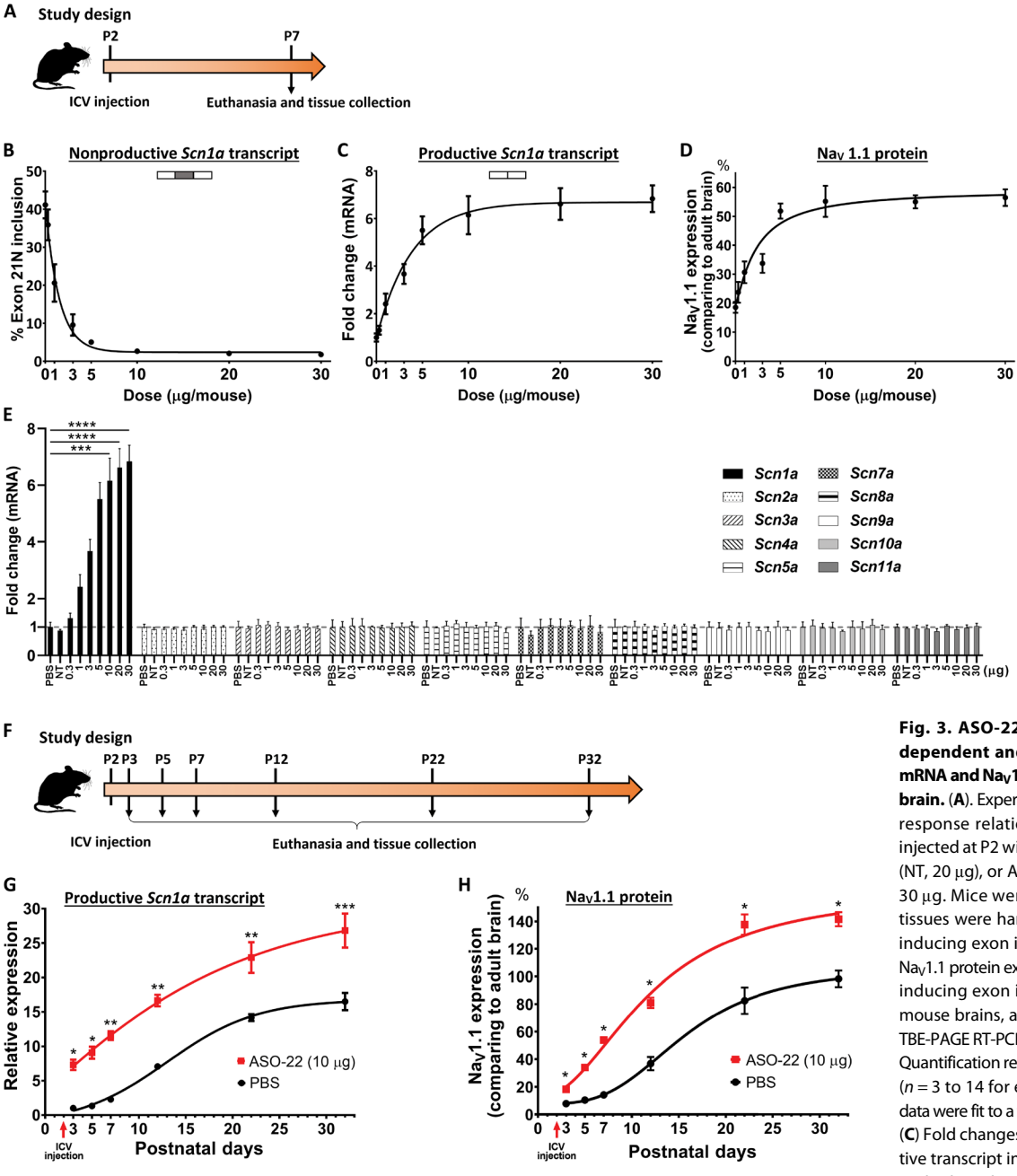

Fig. 3. ASO-22 ICV injection causes dose-dependent and durable increases in *Scn1a* mRNA and $Na_V1.1$ protein expression in mouse brain. (**A**). Experimental design for ASO-22 dose-response relationship in vivo. Mice were ICV-injected at P2 with PBS, a nontarget ASO control (NT, 20 μg), or ASO-22 at 0.3, 1, 3, 5, 10, 20, or 30 μg. Mice were euthanized at P7, and brain tissues were harvested and analyzed for NMD-inducing exon inclusion, *Scn1a* transcript, and $Na_V1.1$ protein expression. (**B**) Percentage of NMD-inducing exon inclusion in *Scn1a* transcript in mouse brains, as quantified by densitometry of TBE-PAGE RT-PCR products (gels shown in fig. S2). Quantification results are presented as mean ± SD ($n = 3$ to 14 for each treatment group). Plotted data were fit to a four-parameter nonlinear curve. (**C**) Fold changes in expression of *Scn1a* productive transcript in mouse brains, as quantified by probe-based qPCR. qPCR results are presented as mean ± SD ($n = 3$ to 14 for each treatment group). Plotted data were fit to a four-parameter nonlinear curve. (**D**) Changes in expression of $Na_V1.1$ protein in mouse brain, as quantified by the Meso Scale Discovery (MSD) method. Quantification results are presented as mean ± SD ($n = 3$ to 8 for each treatment group). Plotted data were fit to a four-parameter nonlinear curve. (**E**) Effect of ASO-22 on expression of the nine VGSC α subunit genes plus Nax (*Scn7a*) expressed in mouse brain. Expression of *Scn1a* productive transcript and the remaining eight VGSC α subunit genes plus Nax (*Scn7a*) in mouse brains after ICV injection of PBS, a nontarget ASO control (NT, 20 μg), or different doses of ASO-22 was measured by probe-based qPCR. Expression of each transcript was first normalized to endogenous *Gapdh* and then compared to PBS injection controls. qPCR assays used here are listed in Materials and Methods. Data are presented as mean ± SD ($n = 3$ to 14 for each treatment group). For comparison of means, Kruskal-Wallis test followed by Dunn's multiple comparisons test were performed. $^{***}P < 0.001$ and $^{****}P < 0.0001$. (**F**) Experimental design for assessment of duration of effect in mouse brains after ICV injection of ASO-22. Mice were ICV-injected with PBS or 10 μg of ASO-22 at P2. Brains of different cohorts were harvested 1, 3, 5, 10, 20, or 30 days after dosing for measurement of *Scn1a* mRNA and $Na_V1.1$ protein expression. (**G**) Quantification of *Scn1a* productive transcript in mouse brains at selected days after injection of 10 μg of ASO-22 at P2. *Scn1a* transcript was first normalized to endogenous *Gapdh* and then compared to mouse brains 1 day after receiving the PBS injection. qPCR results were presented as mean ± SD ($n = 4$ to 9 for each treatment group). Mann-Whitney test was performed to compare means between two groups sampled on the same postnatal day. $^{*}P < 0.05$ and $^{**}P < 0.01$. Plotted data were fit to a four-parameter nonlinear curve. (**H**) Fold changes in expression of $Na_V1.1$ protein in mouse brains at selected days after injection of 10 μg of ASO-22 at P2. $Na_V1.1$ protein expression was quantified by the MSD method. MSD results were presented as mean ± SD ($n = 4$ to 5 randomly selected samples from each treatment group). Mann-Whitney test was performed to compare means between two groups sampled on the same postnatal day. $^{*}P < 0.05$.

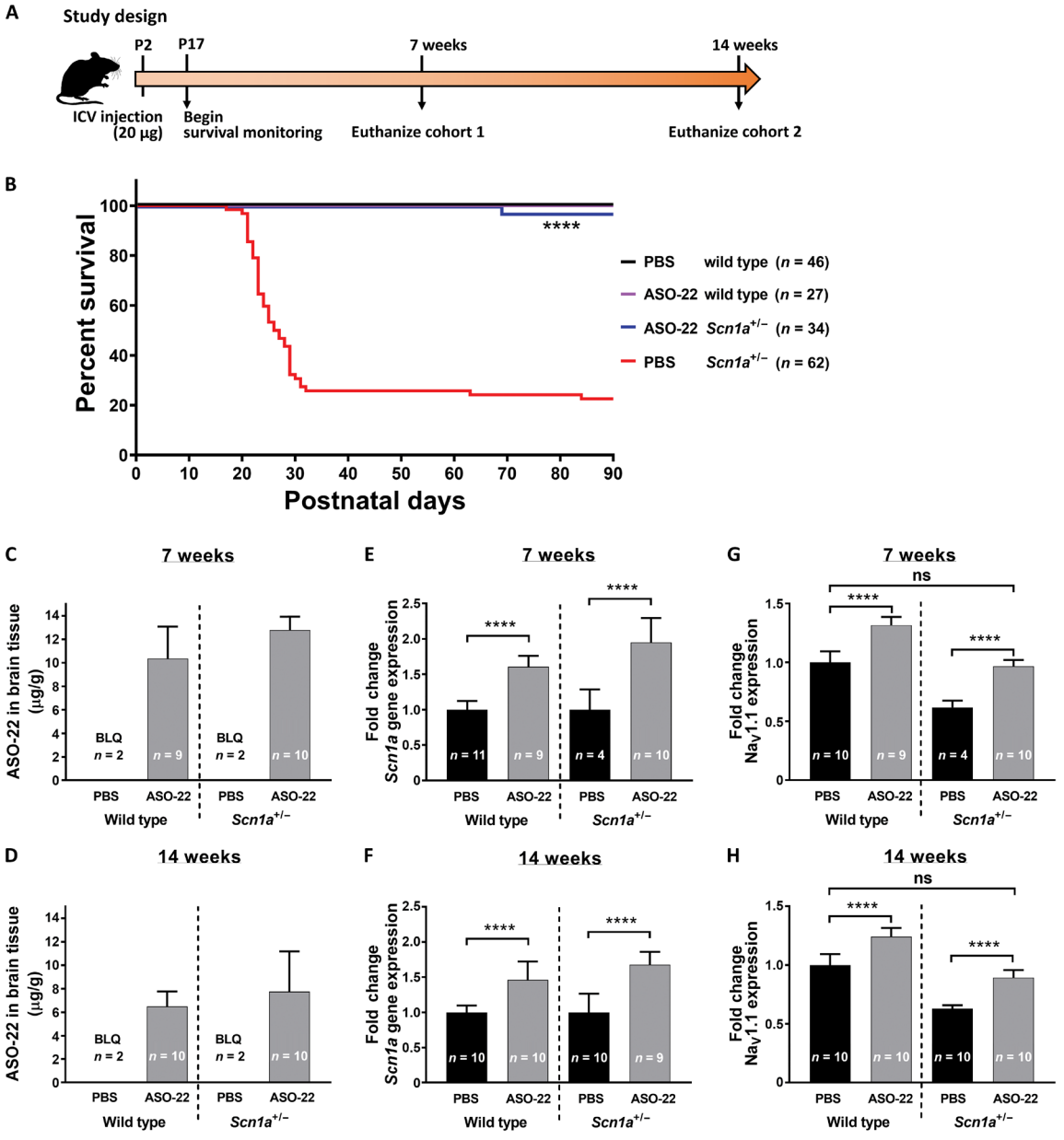

Fig. 4. A single ICV injection of 20 μg of ASO-22 at P2 results in reduced SUDEP incidence and increased $Na_V1.1$ protein expression in DS mice. (**A**) Experimental design for target engagement, pharmacology, and efficacy study in DS and WT mice. DS and WT littermate mice were ICV-injected with a single dose of 20 μg of ASO-22 or PBS at P2 and then genotyped at ~P14. Survival of the mice was monitored until P90. Subgroups of mice of each genotype were euthanized at 7 or 14 weeks, and their brain tissues were harvested and analyzed for ASO exposure, *Scn1a* transcript, and $Na_V1.1$ protein expression. (**B**) Kaplan-Meier curve showing survival of DS and WT littermate mice after a single ICV injection of 20 μg of ASO-22 or PBS at P2. Animals were monitored to P90 for survival. Thirty-three of 34 of ASO-injected DS mice survived to P90 compared with 14 of 62 DS mice in the PBS-treated group. (**C** and **D**) ASO exposure in mouse brains 7 weeks (C) or 14 weeks (D) after ICV injection of 20 μg of ASO-22 at P2, as measured by liquid chromatography–mass spectrometry (LC-MS). BLQ, below the limit of quantification. (**E** and **F**) Expression of *Scn1a* productive transcript in mouse brains 7 weeks (E) or 14 weeks (F) after ICV injection of 20 μg of ASO-22 at P2, as measured by probe-based qPCR. (**G** and **H**) $Na_V1.1$ protein in mouse brains 7 weeks (G) or 14 weeks (H) after ICV injection of 20 μg of ASO-22 at P2, as measured by the MSD method. Two-tailed Student's *t* test was performed to compare means between two groups. For all panels: Quantification results are presented as mean ± SD. ****$P < 0.0001$; ns, no significant change.

Here, we provide preclinical evidence that ICV administration of a TANGO ASO, ASO-22, designed to selectively prevent the inclusion of a naturally occurring NMD exon in human and mouse *Scn1a* transcripts can restore productive *Scn1a* mRNA and $Na_V1.1$ protein expression in *Scn1a*$^{+/-}$ DS mouse brains to WT amounts. The effect of ASO-22 is specific to *Scn1a* and does not alter the expression of other VGSC α subunit genes in cultured cells or in vivo. ASO-22 administration reduces seizure (Fig. 6B) and SUDEP incidence (Figs. 4B and 5B) in the *Scn1a*$^{+/-}$ mouse model of DS with no detectable adverse effects on EEG pattern, generalized behavioral seizures, or survival in similarly treated *Scn1a*$^{+/+}$ littermates, in spite of increased expression of $Na_V1.1$ in the brains of these animals.

There are a number of *SCN1A*-targeted gene therapy approaches being developed for DS. For example, Colasante (*18*) and colleagues recently published a viral, dCas9-based *Scn1a* activation strategy that restored interneuron excitability and attenuated febrile seizures in a DS mouse model. In contrast to viral gene therapy strategies, ASO therapy is reversible, is nonimmunogenic, and is not dependent on gene size (*19*), making this modality well suited for the development of targeted therapies for DS. ASOs delivered directly into the central nervous system have several unique pharmacokinetic

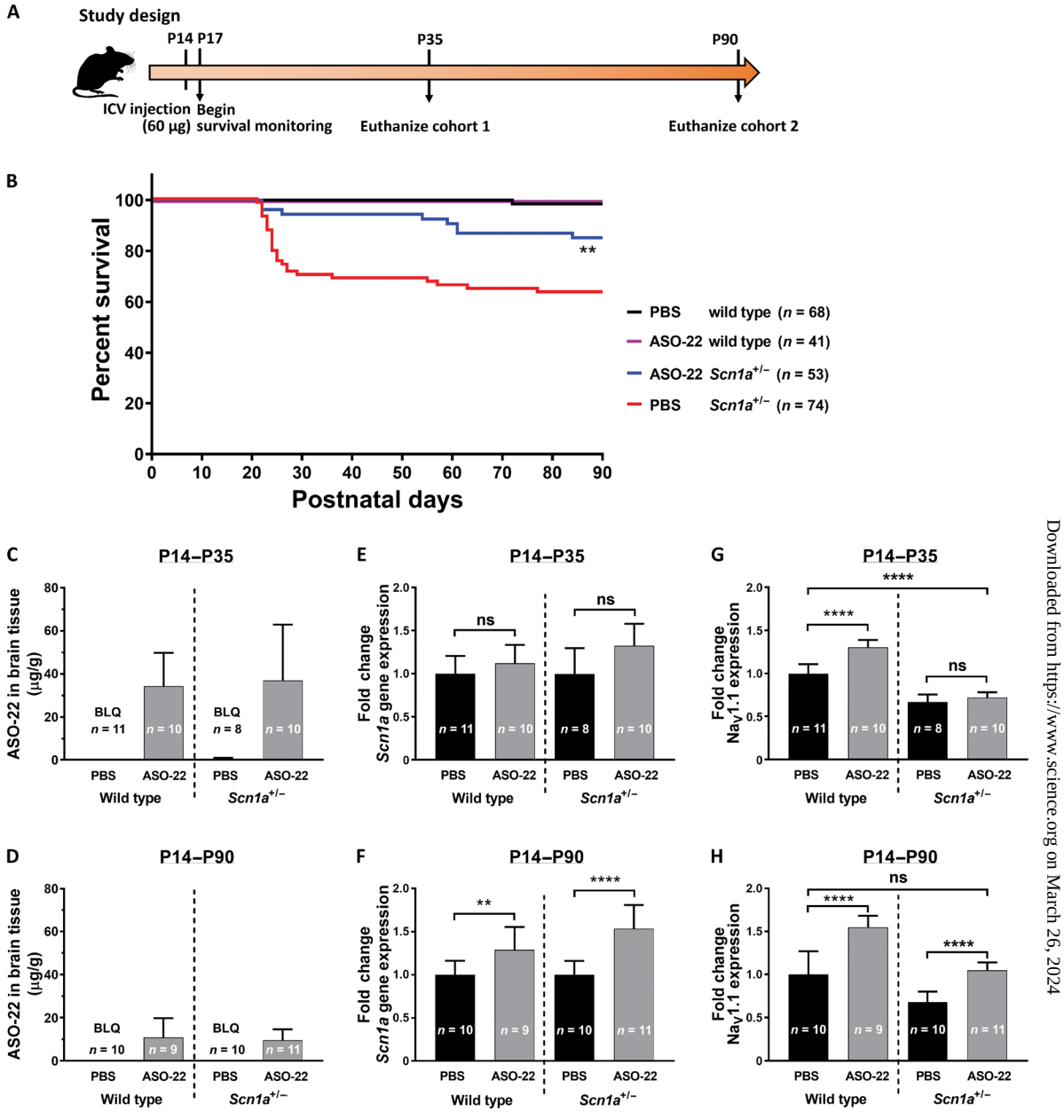

Fig. 5. A single ICV injection of 60 μg of ASO-22 at P14 results in reduced SUDEP incidence and increased $Na_V1.1$ protein expression in DS mice. (**A**) Experimental design for target engagement, pharmacology, and efficacy in DS and WT mice treated with ASO-22 at P14, close to seizure onset. DS and WT littermate mice were ICV-injected at P14 with a single dose of 60 μg of ASO-22 or PBS. Survival of the mice was monitored until 90 days after injection. Cohorts of mice in each group were euthanized at 35 or 90 days, and their brain tissues were harvested and analyzed for ASO exposure, *Scn1a* transcript, and $Na_V1.1$ protein expression. (**B**) Survival of the DS mice and their WT littermates receiving a single bolus ICV injection of 60 μg of ASO-22 or PBS at P14. Animals were monitored out to 90 days for survival. (**C** and **D**) ASO exposure in mouse brains 35 days (C) or 90 days (D) after receiving ICV injection of 60 μg of ASO-22 at P14 as measured by the LC-MS method. BLQ, below the limit of quantification. (**E** and **F**) Expression of *Scn1a* productive transcript in mouse brains 35 days (C) or 90 days (D) after receiving ICV injection of 60 μg of ASO-22 at P14 as measured by probe-based qPCR. (**G** and **H**) $Na_V1.1$ protein in mouse brains 35 days (C) or 90 days (D) after receiving ICV injection of 60 μg of ASO-22 at P14 as measured by the MSD method. Two-tailed Student's *t* test was performed to compare means between two groups. For all panels: Quantification results are presented as mean ± SD. $^{**}P < 0.01$; $^{****}P < 0.0001$; ns, no significant change.

and pharmacodynamic properties, including active uptake, low systemic exposure, long half-lives, accumulation in the nucleus, and gradual release from subcellular depots (*20*). The recent clinical success of nusinersen, an ASO therapy designed to treat pediatric patients with spinal muscular atrophy beginning in infancy, lends further confidence to this approach (*21*).

Our results show that the NMD substrate for ASO-22 is relatively abundant in early postnatal mouse brain. We also detected this substrate in the brain of a DS patient who died of SUDEP, suggesting the possible translatability of our work to humans. Recently, Carvill *et al.* (*22*) showed that patient variants located in the NMD-inducing exon region that we identified caused an increase in NMD-exon inclusion and a reduction of productive mRNA leading to DS. Although this work holds great promise for future therapeutic development of ASOs to treat DS in human patients, important questions remain that cannot be answered using currently available mouse models. First, there is a general lack of agreement in the field about how best to correlate mouse age with human age. Understanding how the time course of DS in mice, where seizures begin at ~P17 to P18 with SUDEP beginning around ~P22, relates to the time course of disease in patients with DS, in which the first seizure usually occurs during year 1 with cognitive impairment evident by

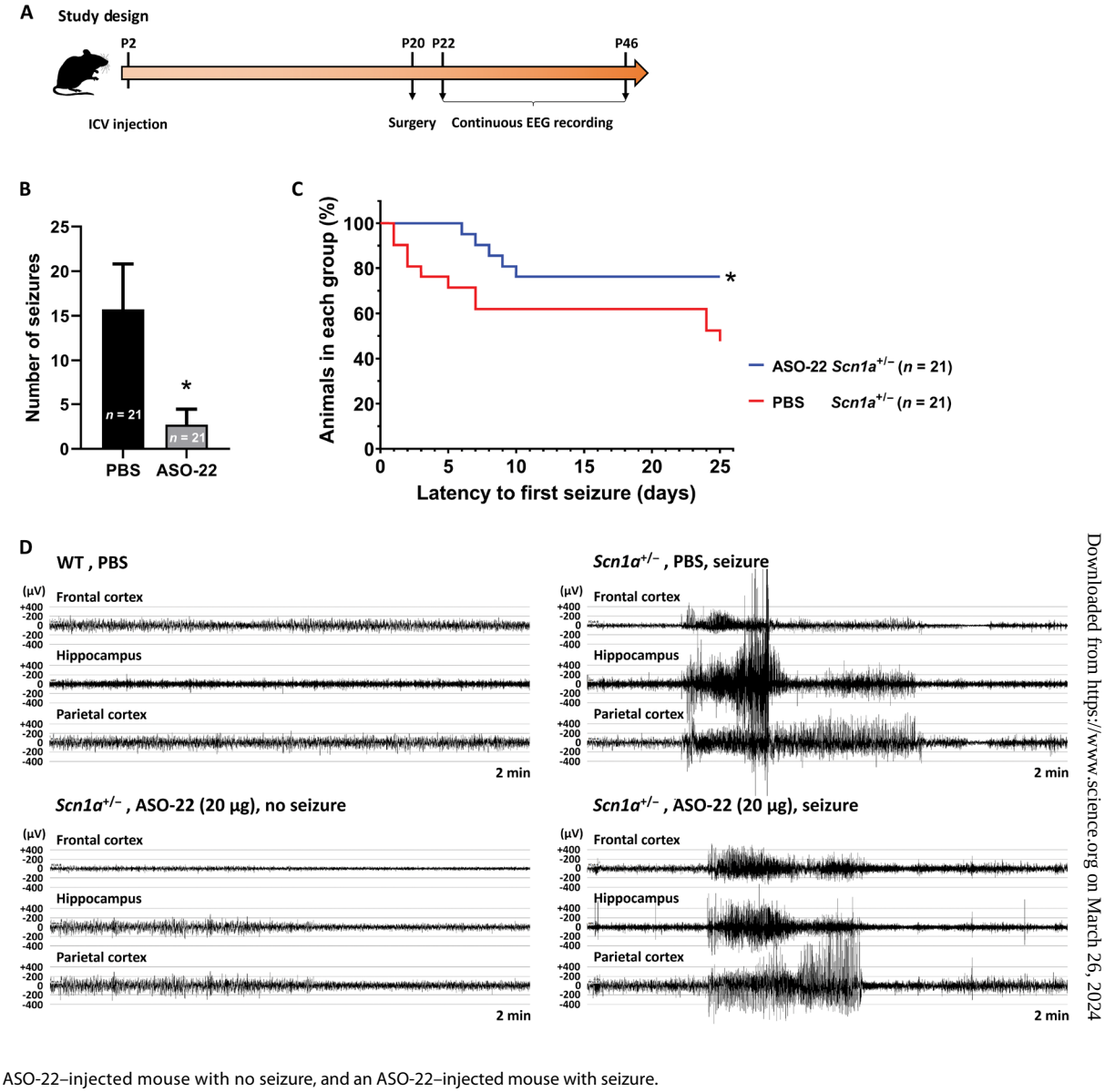

Fig. 6. A single ICV injection of 20 µg of ASO-22 at P2 reduces seizures and prolongs latency to first seizure in DS mice. (**A**) Experimental design for the EEG seizure monitoring study in DS mice ($n = 21$ per group) and their WT littermates ($n = 11$ to 12 per group). Mice received a 20-µg ICV injection of ASO-22 or PBS vehicle at P2, underwent surgery for EEG head mounts at P20, and were continuously monitored by EEG from P22 to P46. (**B**) Effect of ASO-22 on total number of spontaneous seizures (generalized and focal) recorded between P22 and P46 in DS mice dosed with PBS ($n = 21$) or ASO-22 ($n = 21$). Quantification results are presented as mean ± SEM. Mann-Whitney test was performed to compare means between two groups. *$P < 0.05$. (**C**) Effect of ASO-22 on the latency to the first recorded seizure between P22 and P46 in DS mice dosed with PBS ($n = 21$) or ASO-22 ($n = 21$). *$P < 0.05$. (**D**) Representative EEG traces from three brain regions (frontal cortex, hippocampus, and parietal cortex) during a seizure recorded in a PBS-injected WT mouse, a PBS-injected DS mouse with seizure, an ASO-22–injected mouse with no seizure, and an ASO-22–injected mouse with seizure.

year 5, remains unclear. In DS mouse models, the time window between seizure onset and SUDEP is as short as 3 to 5 days, a period that is insufficient to be able to investigate critical issues such as the relationship between drug administration, symptom onset, and death. In addition, the penetrance of the DS phenotype in mouse models is variable and strain dependent. The *Scn1a*$^{+/-}$ mice in this study have the identical (129S × C57BL/6J) F1 genetic background, but only 50% of the mice, on average, develop spontaneous, generalized seizures and SUDEP. The remaining animals have minimal behavioral seizure phenotypes and live normal life spans (*13*). It is not clear how this aspect of the model relates to human DS. Although translatability of mouse models to humans is never certain, the DS mouse model does recapitulate key hallmarks of DS that are effectively controlled using TANGO ASOs. There was no impact of ASO-22 on expression of $Na_V1.1$ protein after injection at P14 when the data were evaluated at P35. We do not have a clear explanation for this result, except that treatment at P14 was clearly not as robust as was observed when animals were treated at P2. It is possible that a 60-µg dose at this developmental time point, when the mouse brain is near adult size, may not be sufficient. Alternatively, developmental changes in the mouse brain may limit the therapeutic window for ASO administration in this model. Further studies using alternative models with longer time periods between seizure onset and SUDEP will be needed to better understand these findings.

An important point to consider regarding the future clinical utility of the TANGO approach in DS is its limitation to patients with *SCN1A* variants that result in $Na_V1.1$ haploinsufficiency, for example, truncating, nonsense, or frameshift variants, and partial or whole gene deletions (*23*). Because truncation variants have been identified in >50% of patients with DS (*23*–*26*), the TANGO approach is predicted to provide therapeutic benefit to a wide range of individuals. However, TANGO may be contraindicated for some

patients with missense *SCN1A* variants that result in the generation of $Na_V1.1$ polypeptides that have maladaptive gain-of-function or dominant negative effects (*27*, *28*), as TANGO-mediated increases in protein expression may increase disease severity. However, according to published cases, about 80% of missense variants in patients with DS that have been evaluated are loss of function resulting in haploinsufficiency (*25*). For future clinical trials using this approach, patients should be genetically screened and those with known maladaptive gain-of-function or dominant negative mutations excluded.

In summary, the current studies demonstrate target engagement, pharmacology, and efficacy using the TANGO approach to selectively increase *Scn1a* gene and $Na_V1.1$ protein expression in a DS mouse model. This strategy shows promise for ASO therapy to be a precise, disease-modifying treatment for patients with DS and warrants preclinical testing to further evaluate the safety and efficacy of this molecule.

MATERIALS AND METHODS

Study design

In this study, we tested a mechanism (TANGO) of using ASOs to specifically increase the expression of the *SCN1A* gene and its protein product, $Na_V1.1$, using in vitro and in vivo systems. We further assessed the potential of using the TANGO approach to modify disease phenotypes in a mouse model of DS. The designated end points were selected prospectively to assess target engagement/pharmacology (*SCN1A* mRNA/$Na_V1.1$) and/or efficacy (survival and seizures). ASO screens in vitro were done in singlicate wells and designed to identify trends to select molecules for further, more rigorous, study. Additional studies were conducted in biological replicates using cell densities previously optimized for either gymnotic or nucleofection-mediated uptake of ASOs. Small numbers of animals were enrolled for the natural history tracking of *Scn1a* gene expression in WT mice during postnatal development in an effort to conserve animal usage. For pharmacology and efficacy studies, litters of mice were randomly assigned to treatment groups and dosed with the same compound (at either P2 or P14) to minimize stress of marking the animals before weaning. For the efficacy studies, pilot natural history studies in the DS mouse model and power analyses helped to determine the number of animals necessary for the efficacy studies a priori. Researchers were not blinded to the in vitro experiment condition but were blinded to genotype and treatment condition in the in vivo experiments. No data were excluded from any of the experiments reported in this study.

ASO gymnotic (free) uptake by ReNcells VM

All ASOs used for screens were purchased from Integrated DNA Technologies (IDT) or Bio-Synthesis Inc, with sequences referenced in PCT/US2018/48031; WO/2019/040923. Before proceeding with the gymnotic uptake, ASOs were dissolved in nuclease-free H_2O and the concentrations in solution were determined by OD_{260nm} (optical density at 260 nm) absorbance. ReNcells VM (EMD Millipore, SCC008) were grown in laminin-coated flasks in complete Neural Stem Cell (NSC) medium. Complete NSC medium was prepared by supplementing maintenance medium (Millipore, SCM005) with basic fibroblast growth factor (EMD Millipore, GF003) and epidermal growth factor (EMD Millipore, GF144) to a final concentration of 20 ng/ml each. Cells were detached from the flask by incubation with Accutase (Millipore, SCR005), resuspended in prewarmed maintenance medium, and pelleted at 300*g* by centrifugation. The supernatant was removed by aspiration, and the cells were resuspended in complete NSC medium to ~6×10^5/ml. Cell suspension (0.5 ml) (~3×10^5 cells) was added to each well of an Ultra-Low Attachment Costar 24-well plate (Corning, 3473) containing ASO. The cells were mixed gently with ASO and then incubated at 37°C, 5% CO_2 for 72 hours before harvesting. In some cases, as indicated, dimethyl sulfoxide or CHX (at a final concentration of 50 ng/ml; Cell Signaling Technology, 21125) was added to the cell culture 3 hours before harvest.

Nucleofection of ReNcells VM

ReNcells were resuspended in Nucleofector Solution SF (Lonza, V4XC-2024) to ~1.5×10^7/ml. Eighteen microliters of the suspension (~3×10^5 cells) was mixed with 2 μl of ASO (at varying concentrations) in an Eppendorf tube. The mixture was transferred to a well of a 16-well Nucleocuvette Strip (Lonza) and electroporated with a 4D-Nucleofector (Lonza), using Nucleofector program DS-150. Eighty microliters of prewarmed complete NSC medium was added to the well immediately after electroporation. The cells in each well were mixed by gentle pipetting, then transferred to a well of a 24-well ultra-low attachment plate containing 0.5 ml of complete NSC medium. The cells were incubated at 37°C, 5% CO_2 for 72 hours before harvesting.

Extraction of total RNA from cultured ReNcells

Total RNA was extracted from cultured ReNcells using the Qiagen RNeasy Kit (Qiagen, 74106). Cells grown in ultra-low attachment wells were carefully transferred into a 1.5-ml Eppendorf tube, pelleted by 300*g* centrifugation for 3 min, and lysed with 300 μl of buffer RLT supplemented with 1% β-mercaptoethanol. Cell lysates were transferred to 1.5-ml Eppendorf tubes. An equal volume of 70% ethanol (300 μl) was added to each cell lysate and mixed. The mixture (600 μl) was passed through an RNeasy column by centrifugation at 14,000*g* for 1 min. Each column was washed sequentially with 700 μl of buffer RW1 and 700 μl of buffer RPE. Each empty column was centrifuged again after the final wash for 1 min at top speed. RNA was eluted from the column by 40 μl of ribonuclease (RNase)–free water.

Animals

Mouse studies conducted at Stoke Therapeutics Inc. were performed under protocols approved by the Institutional Animal Care and Use Committee (IACUC) of NeoSome Life Sciences, LLC and were in accordance with the National Institutes of Health (NIH) *Guide for the Care and Use of Laboratory Animals*. Mouse studies conducted at University of Michigan were performed in compliance with protocols approved by University of Michigan IACUC and were in accordance with the policies of the NIH *Guide for the Care and Use of Laboratory Animals*. Mouse studies conducted at PsychoGenics were performed in compliance with protocols approved by PsychoGenics' IACUC and aligned with the Association for Assessment and Accreditation of Laboratory Animal Care (AAALAC; unit no. 001213) and the Office of Laboratory Animal Welfare (PHS OLAW D16-00732 [A4471-01]) assurances. *Scn1a*^{tm1Kea} mice, containing a deletion of exon 1 of *Scn1a*, were a gift from the laboratory of J. Kearney at Northwestern University. The *Scn1a*^{tm1Kea} colony was maintained by breeding heterozygous (129S6.*Scn1a*$^{+/-}$) animals to 129S6/SvEvTac mice (Taconic, #129SVE). For all experiments, C57BL/6J (JAX, #00064) mice were crossed to 129S6.*Scn1a*$^{+/-}$ mice to generate F1 offspring. Genotyping of F1 pups was performed by

PCR amplification of mouse genomic DNA. Primers used in genotyping were 5′-AGTCTGTACCAGGCAGAACTTG-3′, 5′-CTGTTTGCTCCATCTTGTCATC-3′, and 5′-GCTTTTGAAGCGTGCAGAATGC-3′. The PCR products are 1 kb for the *Scn1a* WT allele and 650 base pairs (bp) for the transgenic allele. All mice were maintained on a 12:12-hour light:dark cycle and had ad libitum access to food and water throughout the experiments. Male and female mice were used in all experiments.

Single bolus ICV injection in neonate mice

Lyophilized ASO was reconstituted in 1× PBS (Thermo Fisher Scientific, 10010023), and the concentration of ASO solution was determined by OD_{260nm} absorbance. For dosing solutions, reconstituted ASO was diluted to the desired concentration in PBS with 0.01% (weight to volume) fast green dye (Sigma-Aldrich, F7252-5G). PBS with 0.01% fast green dye was prepared as the vehicle control. For ICV injection in P2 or P14 mice, pups were immobilized by gentle restraint on a soft tissue padded surface with two fingers. A 33-gauge needle (0.375 inch long, point style 4, 12° beveled; Hamilton, 7803-05) attached to a 5-μl microvolume syringe (Hamilton, 7634-01) was used for the injection. The coordinates of the injection were about 1 mm lateral from the bregma and −2 mm ventral. Two microliters (for the 20-μg dose) or 3 μl (for the 60-μg dose) of ASO or PBS was injected slowly into one cerebral lateral ventricle. Injected mice were quickly returned to the nest and observed daily for survival and signs of stress. Investigators performing the injections were blinded to study material and genotype.

Survival monitoring

Mice were observed daily by an individual blinded to genotype and treatment for survival from P17 to P90. Mice were returned to the housing room at the end of business hours where they were monitored by veterinary staff. Survival data were compiled for each treatment and genotype in GraphPad Prism 8.0 software (GraphPad Software, CA), and survival curves were generated.

Continuous video monitoring of DS mice for spontaneous seizure activity and SUDEP

Mice were observed in a static housing cage from P17 to P35. At P21, mice were weaned and the parents were removed from the observation chamber. Throughout the study, a 12:12-hour light:dark cycle was preserved and University of Michigan Unit for Laboratory Animal Medicine (ULAM) standard chow and water were provided ad libitum. All mice were observed in ULAM standard housing conditions including housing density, nesting material, and diet. Mice were not single-housed. Videos were recorded using OmniPlex D software and hardware acquired from Plexon Inc. in Dallas, Texas, USA and securely stored under password protection at University of Michigan. Videos were recorded continuously during the entire observation period, with infrared lights illuminating the arena during the dark cycle. Cameras were oriented to provide full field of view of the observation chamber from a side angle. This setup allowed optimal viewing to ensure that any generalized seizures would not be occluded and that any terminal events would be captured accurately. Mice that died during the study were removed from the arena during daily husbandry checks. Each video was viewed and analyzed manually by an investigator blinded to genotype and treatment. Seizures were defined as visualized general tonic-clonic presenting with running and jumping of the affected mouse.

EEG recordings

Single-housed mice were surgically implanted at P19 to P20 with an 8201-EEG Headmount (Pinnacle Technology Inc.), which consisted of supradural screw electrodes (0.10 to 0.12 inches) in frontal and parietal cortices and an indwelling insulated, stainless steel wire electrode in the hippocampus. Mice were allowed to recover for 48 hours before recording began. Electrodes were recorded simultaneously, and each electrode was configured to provide differential measurements between the electrode and the common reference (or ground), which was a screw placed in the cerebellum. EEGs were recorded continuously using the Pinnacle Technology 8206 data conditioning and acquisition system. Electrographic seizures were manually identified by visualizing data offline using a 2-min sliding window. Seizures were readily identifiable from the typically artifact-free (very little movement artifact) traces, and all incidences marked as a seizure clearly exhibited spikes greater than background EEG for greater than 10 s with a clear beginning and end of ictal activity. Recordings were made continuously from P22 to P46. In most cases, seizures were generalized (detected in all three brain regions simultaneously) so seizure counts were presented as a combination of all three brain regions [generalized seizures were each counted as one over the time of recording] (each 24-hour recording). The latency to first seizure was calculated as the first day a seizure occurred from the start to the end of the EEG recordings (P22 to P46). The latency to first seizure was based on the presence of a seizure occurring in any of the three brain regions. All animals were censored on day 25 of EEG recording, and thus, if a mouse did not have any seizures within these 25 days, the mouse received a latency score of 25. The number of mice having 0, 1, or 2 or more seizures ("focal" or "generalized") was quantified and plotted as a bar graph. All EEG studies were performed at PsychoGenics Inc., and the personnel were blinded to the treatment groups.

Tissues

Mouse: A coronal section (~1 mm, ~30 mg) of the mouse brain close to the bregma was cut with two juxtaposed razor blades to obtain tissue for total RNA extraction. Two additional adjacent coronal sections immediately rostral and caudal to the first were also collected for assessment of ASO exposure and $Na_V1.1$ protein expression, respectively. Coronal sections were snap-frozen in liquid nitrogen and stored in a −80°C freezer until analysis. Human: Healthy human cerebral cortex was obtained from a 19-year-old Caucasian female donor (Cureline Inc., ID: S9-5 C). Total RNA from a DS patient who died of SUDEP (IE 1201, NM_001202435.1:c.5010_5013delGTTT, p.Phe1671ThrfsTer8, 5010) was obtained from A. Goldman at Baylor College of Medicine, Center for SUDEP Research. Monkey: Cynomolgus monkey (*Macaca fascicularis*) brain tissues were purchased from Toxikon Inc. Rat: Sprague-Dawley rat brain tissues (catalog no. RATO0BRAIN 1805435) were purchased from BioIVT.

Extraction of total RNA from brain tissue

Total RNA was extracted from brain tissue using the Qiagen RNeasy Kit (Qiagen, 74106). Brain tissue (~30 mg) was mixed with 400 μl of QIAzol reagent (Qiagen, 79306) and ~0.1 ml of zirconium oxide beads (Next Advance, ZROB05 and ZROB10) in a sterile microcentrifuge 1.5-ml RINO tube (Next Advance, TUBE1R5-S). Brain tissue was then homogenized in a Bullet Blender Storm Bead Mill tissue homogenizer (Next Advance, BBY24M) at 4°C and speed setting 8, for 4 min. The homogenate was briefly centrifuged at 13,000*g* to precipitate

insoluble debris. The supernatant (~300 μl) was transferred to a new tube and mixed with 400 μl of fresh QIAzol and 250 μl of chloroform. The mixture was vortexed vigorously for 15 s, incubated at room temperature for 2 to 3 min, and centrifuged at 13,000*g* for 15 min at 4°C. The upper aqueous layer (~340 μl) was transferred to a new tube. The supernatant was mixed with one volume (340 μl) of 70% ethanol, incubated at room temperature for 10 min, and passed through an RNeasy column by centrifugation at 13,000*g* for 1 min. The column was washed sequentially with 700 μl of buffer RW1 and 700 μl of buffer RPE. Each empty column was centrifuged at full speed for 1 min after the last wash and dried at room temperature for 5 min. Total RNA was eluted from the column with 50 μl of RNase-free water. RNA concentrations were determined by OD_{260nm} absorbance.

cDNA synthesis

Complementary DNA (cDNA) was synthesized using the ImProm-II reverse transcriptase kit (Promega, A3803). One microgram of the RNA template was mixed with 0.5 μg of oligo(dT) in a total volume of 11 μl. The mixture was incubated at 70°C for 6 min and quickly chilled to 4°C. Master mix (9 μl) containing $MgCl_2$, deoxynucleotide triphosphates (dNTPs), and ImProm-II reverse transcriptase was added to the RNA and oligo(dT) mixture, and the reaction was carried out as follows: 25°C annealing for 5 min, 42°C extension for 60 min, 70°C heat inactivation for 15 min, followed by 4°C hold.

Reverse transcription polymerase chain reaction

PCRs were prepared by mixing the following reagents in a 0.2-ml PCR tube: 1× AmpliTaq Gold 360 Master Mix (Applied Biosystems, 4396790), forward and reverse primers (0.4 μM each), cDNA template (1 μl), and nuclease-free H_2O in a total volume of 25 μl. The PCR cycle conditions were 95°C for 9 min for 1 cycle; 95°C for 30 s, 56°C for 30 s, 72°C for 75 s for 30 cycles (for *Scn1a*) or 95°C for 30 s, 56°C for 30 s, 72°C for 60 s for 25 cycles (for *RPL32* or *Gapdh*); 72°C for 5 min. PCR products were separated on a 5% tris-borate EDTA (TBE) polyacrylamide gel (Criterion Precast Gel, Bio-Rad, 3450049) by electrophoresis. The gel was stained with SYBR Safe Dye (1:10,000 dilution, Thermo Fisher Scientific, S33102) for 30 min and scanned using a Typhoon 9500 laser scanner (GE Healthcare Life Sciences).

The following primers were used: human *SCN1A* transcript (exons 20 to 23), 5′-ATTGTTGATGTTTCATTGGTCAGTTTAACA-3′ (forward) and 5′-GAAGAAGGACCCAAAGATGATGAAAATA-3′ (reverse); monkey *SCN1A* transcript (exons 20 to 23), 5′-ATTGTTGATGTTTCACTGGTCAGTTTAACA-3′ (forward) and 5′-GAAGAAGGACCCAAAGATGATGAAAATA-3′ (reverse); mouse *Scn1a* transcript (exons 21 to 24), 5′-CAGTTTAACAGCAAATGCCTTGGGTT-3′ (forward) and 5′-AAGTACAAATACATGTACAGGCTTTCCTCATACTTA-3′ (reverse); rat *Scn1a* transcript (exons 21 to 24), 5′-CAGTTTAACAGCAAATGCCTTGGGTT-3′ (forward) and 5′-AGGTACATGTACAGGCTTTCCTCATACTTA-3′ (reverse); human *RPL32*, 5′-AGAGGCATTGACAACAGGGTT-3′ (forward) and 5′-GTGAGCGATCTCGGCACAG-3′ (reverse); mouse *Gapdh*, 5′-AGGTCGGTGTGAACGGATTTG-3′ (forward) and 5′-GGGGTCGTTGATGGCAACA-3′ (reverse).

Predicted molecular weights of the RT-PCR products for *SCN1A mRNA*: for human and monkey, productive transcript (containing exons 20, 21, 22, and 23): 549 bp; nonproductive transcript (containing exons 20, 20N, 21, 22, and 23): 613 bp; for mouse and rat, productive transcript (containing exons 21, 22, 23, and 24): 498 bp; nonproductive transcript (containing exons 21, 21 N, 22, 23, and 24): 562 bp.

SYBR green qPCR assay

SYBR green qPCR was prepared by mixing the following reagents in each well of a MicroAmp Optical 384-well reaction plate (Applied Biosystems, 4309849): 1× Power SYBR Green PCR Master Mix (Applied Biosystems, 4367659), forward and reverse primers (4 μM, 1 μl each), cDNA template (1 μl), and nuclease-free H_2O in a total volume of 10 μl. The PCR and optical reading of the plate were performed using a QuantStudio 5 thermocycler. qPCRs were performed in triplicate for each sample. SYBR green qPCR cycle conditions were 50°C for 2 min for 1 cycle; 95°C for 10 min for 1 cycle; 95°C for 15 s, 60°C for 1 min for 40 cycles; 95°C for 15 s, 60°C for 1 min, then the temperature was slowly raised to 95°C at a rate of 0.075°C per second for melt curve determination.

The following primers were used: human *Scn1a* productive transcript, 5′-ATTGTTGATGTTTCATTGGTCAGTTTAACA-3′ (forward) and 5′-GGCATTCACAACCACCCTCATC-3′ (reverse); human *RPL32* transcript, 5′-AGAGGCATTGACAACAGGGTT-3′ (forward) and 5′-GTGAGCGATCTCGGCACAG-3′ (reverse).

Probe-based qPCR

Probe-based qPCR was prepared by mixing the following reagents in each well of a 384-well plate (Applied Biosystems, 4309849): cDNA (1 μl), 1× TaqMan Gene Expression Master Mix (Applied Biosystems, 4370074), 1× primers/probe mix, and nuclease-free H_2O, to a total volume of 10 μl. The PCR and optical reading of the plate were performed with a QuantStudio 5 thermocycler (Thermo Fisher Scientific). qPCRs were performed in triplicate for each sample. qPCR cycle conditions were 50°C for 2 min for 1 cycle, 95°C for 10 min for 1 cycle, 95°C for 15 s, 60°C for 1 min for 40 cycles. ΔC_t was calculated by subtracting the average C_t (of three technical replicates) of the reference gene from the average C_t (of three technical replicates) of gene of interest for each sample. The ΔC_t values were converted into $\Delta\Delta C_t$ values by subtracting the average ΔC_t value of control samples from the ΔC_t of the test samples. The $\Delta\Delta C_t$ was then converted into $2^{-\Delta\Delta Ct}$ for fold change of the gene expression.

qPCR assay for human *SCN1A* productive transcript: forward primer, 5′-TGGGTTACTCAGAACTTGGA-3′; reverse primer, 5′-GCATTCACAACCACCCTC-3′; probe, 5′-/56-FAM/CAAATCTCT/ZEN/CAGGACACTAAGAGCTCTGAGAC/3IABkFQ/-3′ (20× assay contains 0.5 μM of the primers each and 0.25 μM of the probe).

Hs01109871_m1 for human *SCN2A* (Thermo Fisher Scientific), Hs00366913_m1 for human *SCN3A* (Thermo Fisher Scientific), Hs00274075_m1 for human *SCN8A* (Thermo Fisher Scientific), Hs00161567_m1 for human *SCN9A* (Thermo Fisher Scientific), Hs00851655_g1 for human *RPL32* (Thermo Fisher Scientific), Hs03929097_g1 for human *Gapdh* (Thermo Fisher Scientific), Mm00450583_mH for mouse *Scn1a* productive transcript (Thermo Fisher Scientific), Mm.PT.58.32955693 for mouse *Scn2a* (IDT), Mm.PT.58.5993740 for mouse *Scn3a* (IDT), Mm.PT.58.8823368 for mouse *Scn4a* (IDT), Mm.PT.58.30418114 for mouse *Scn5a* (IDT), Mm.PT.58.13836045 for mouse *Scn7a* (IDT), Mm.PT.58.31697139 for mouse *Scn8a* (IDT), Mm.PT.58.12227752 for mouse *Scn9a* (IDT), Mm.PT.58.9384636 for mouse *Scn10a* (IDT), Mm.PT.58.43684449 for mouse *Scn11a*. (IDT), and Mm99999915_g1 for mouse *Gapdh* (Thermo Fisher Scientific).

Total protein preparation and normalization

Brain tissue was homogenized in radioimmunoprecipitation assay (RIPA) buffer (Thermo Fisher Scientific, 89901) (for immunoblotting) or a lysis buffer containing 1× tris-buffered saline, 1% Triton X-100, 0.5% NP-40, 0.25% Na-deoxycholate, and 1 mM EDTA (pH7.4) [for the Meso Scale Discovery (MSD) assay] with a motor-driven Teflon-coated mortar and pestle (Thomas Scientific, 3431D88) at speed of 740 rpm for 30 strokes. The lysate was cleared by centrifugation at 16,000*g*, 4°C, for 15 min. The protein concentration of the tissue lysate was measured with the bicinchoninic acid (BCA) assay (Thermo Fisher Scientific, 23227) after the manufacturer's protocol. The protein concentration of the brain lysate was adjusted to 4 mg/ml with RIPA buffer or MSD lysis buffer.

Immunoblotting

Protein lysates were mixed with one-third volume of 4× Laemmli loading buffer (Alfa Aesar, J60015), loaded into wells of a precast TGX acrylamide gradient gel (Bio-Rad, 5671124), and electrophoresed at 120 V for 90 min. The separated proteins were transferred to a 0.2-μm nitrocellulose membrane (GE Healthcare Life Sciences, 10600004). The membrane was stained with Ponceau S staining solution and scanned with a Canon 9000F Mark II scanner. The image of Ponceau S–stained total protein was used as loading control. The membrane was then destained with tris-buffered saline with 0.1% Tween 20 (TBS-T) and blocked with 1% ECL Prime blocking reagent (GE Healthcare Life Sciences, RPN418V). Primary antibody incubation was performed at 4°C overnight. The membrane was washed with TBS-T and incubated with horseradish peroxidase (HRP)–conjugated secondary antibody at room temperature for 2 hours. ECL Plus Western Blotting Substrate (Thermo Fisher Scientific, 32132) was used for signal development, and the immunoblot images were captured with a Typhoon 9500 laser scanner. Antibodies used in this study were anti-$Na_V1.1$ (rabbit polyclonal, Alomone, ASC-001), anti-$Na_V1.1$ (mouse monoclonal, NeuroMab, 75-023) (see validation of the two anti-$Na_V1.1$ antibodies in fig. S8), anti-rabbit immunoglobulin G (IgG)–HRP (Santa Cruz Biotechnology, sc-2004), and anti-mouse IgG-HRP (goat polyclonal, Santa Cruz Biotechnology, sc-2005).

Densitometry analysis

Scanned images were imported into MultiGauge V2.3 software (Fujifilm). Areas of interest were selected with the rectangle selection tool. The optical densitometry of the selected areas was measured and exported as 16-bit grayscales. The grayscales were background-subtracted and normalized to the loading control (*Gapdh* for mRNA and Ponceau staining for protein) for the same sample. Expression of mRNA or protein was compared to the reference or control samples as the ratio of normalized grayscales.

Sequence analysis

PCR products were purified with a QIAquick PCR purification kit (Qiagen, 28104) after the manufacturer's instructions. Purified PCR products were sequenced with a MinION portable DNA/RNA sequencing device (Oxford Nanopore Technologies), and alternative splicing events of the *SCN1A* gene were identified and characterized by aligning the sequencing results with the reference human genomic sequence assembly GRCh38/hg38. Homologous sequences of the human *SCN1A* gene were identified by performing nucleotide BLAST on the National Center for Biotechnology Information (NCBI) website.

Quantification of $Na_V1.1$ protein in mouse brain

Quantification of $Na_V1.1$ protein in mouse brain was performed using the MSD method. MULTI-ARRAY 96 small spot goat anti mouse (GAM) plates (MSD, L45MA-2) were blocked with 5% MSD blocker B (MSD, R93BB-2) prepared in TBS-T, 100 μl per well, under constant shaking for 1 hour. MSD blocker B was tapped out from the GAM plates, and the wells were coated with capture antibody (0.95 mg/ml, diluted to 1:200 in 5% block B, NeuroMab, 75-023), 25 μl per well, under constant shaking for 4 hours. The capture antibody was tapped out from the GAM plates, and the wells were washed three times with TBS-T (150 μl per well). MSD standards were prepared by diluting adult mouse whole brain lysate with liver lysate. The protein concentration of all standards was kept at 4 mg/ml. Twenty-five microliters of standard or sample lysate (4 mg/ml) was added to GAM plate wells in duplicate. The plates were sealed and incubated overnight at 4°C under constant shaking. The contents were tapped out, and wells were washed three times with TBS-T (150 μl per well). Twenty-five microliters of detection antibody (0.6 mg/ml, diluted 1:250 in 5% block B, Alomone, ASC-001) was added to each well and incubated at room temperature for 2 hours under constant shaking. The detection antibody was tapped out, and wells were washed three times with TBS-T (150 μl per well). Twenty-five microliters of sulfo-tagged anti-rabbit antibody (0.5 mg/ml, diluted 1:250 in 5% block B, MSD, R32AB-1) was added to each well and incubated at room temperature for 1 hour under constant shaking. The contents were tapped out, and wells were washed five times with TBS-T. One hundred fifty microliters of 1× MSD read buffer T (diluted in dH_2O) was added to each well. The plates were read immediately with the Meso QuickPlex SQ 120 machine. The MSD signals for each standard were read from duplicate wells, imported to GraphPad Prism 8.0 software, and fit to a nonlinear, quadratic (second-order) polynomial regression curve. The concentration of $Na_V1.1$ in each sample was interpolated using the standard curve.

Measurement of ASO exposure in brain tissues with LC-MS

Standards for ASO exposure were prepared by spiking matrix made from mouse brain tissue with known quantities of ASO. Mouse brain matrix was prepared by homogenizing brain tissue in lysis buffer containing 2.5% IGEPAL, 0.5 M NaCl, 5 mM EDTA, 50 mM tris (pH 8.0), and proteinase K (250 μg/ml) with a motor-driven Dounce homogenizer (Thomas Scientific, 3431D76) on ice. Brain samples were weighed and homogenized the same way as the standards. An internal standard (a different oligonucleotide) was added to all the standards and samples at a concentration of 25 μg/g of brain tissue.

ASOs were extracted from brain lysates using the Clarity OTX solid phase extraction kit (Phenomenex), following the manufacturer's protocol. LC-MS analyses were performed using a Q-Executive mass spectrometer (Thermo Fisher Scientific) coupled with a Vanquish HPLC system (Thermo Fisher Scientific). Three microliters of the reconstituted extraction solution was injected onto Waters ACQUITY UPLC Oligonucleotide BEH C18 Column (130 Å,1.7 μm, 2.1 × 50 mm) at 80°C using mobile phase A (200 mM hexafluoroisopropanol and 8 mM triethylamine) and mobile phase B (methanol) at a flow rate of 0.3 ml/min. The LC gradients measured by

mobile phase B were 0 to 2 min (18%), 2.0 to 6 min (80%), 6.0 to 6.5 min (90%), 8 to 9 min (18%), and 9 to 12.0 min (18%). The effluent from the LC column was introduced into the ion source of the Q-Exactive mass spectrometer operated in negative mode at a spray voltage of 2.57 kV, with sheath and auxiliary gasses set at 45 and 15 arbitrary units, respectively. ASO and the positive control were detected by targeted single ion monitor *m/z* (mass/charge ratio) scan mass analysis by Orbitrap detector with negative ion mode. Xcalibur software (version 4.0.27 10, Thermo Fisher Scientific) was used for data capture and to calculate peak areas and peak area ratios of analytes (ASO and the positive control) to internal standard. ASO contents in brain samples were interpolated against the standard curve and were normalized to the internal standard.

Statistical analyses

Each set of data is presented as the mean ± SD or SEM, with *n* equal to the number of biological repeats for in vitro experiments or independent samples from individual animals. For comparison of means between two independent groups, two-tailed Student's *t* test was performed. Before performing the Student's *t* test, however, the Shapino-Wilk test was performed to determine whether the data within each group follow the normal (Gaussian) distribution. Homogeneity of variance between groups was tested by the *F* test. If variance between two groups is not the same or the data do not follow normal distribution, the Mann-Whitney nonparametric test was used to compare the difference between the two groups. For comparison of means between three or more independent groups, Kruskal-Wallis test was performed followed by Dunn's multiple comparisons test. Regression analysis was performed to assess *Scn1a* gene expression during postnatal development and for dose-response relationship establishment. Kaplan-Meier (Wilcoxon) plots were used to analyze survival and latency of first seizure in DS model animals. Seizure count data were analyzed with Mann-Whitney test. Data representing the number of mice having 0, 1, or 2+ seizures were analyzed with Fisher's Exact test. Statistical significance for all experiments was defined as $P < 0.05$. All analyses were performed using the GraphPad Prism 8.0 software (GraphPad Software).

SUPPLEMENTARY MATERIALS

stm.sciencemag.org/cgi/content/full/12/558/eaaz6100/DC1

Fig. S1. A control ASO showed dose-responsive effect on SMN2 transcript splicing in ReNcells.

Fig. S2. Dose-dependent effects of ASO-22 on expression of *Scn1a* gene in ICV-injected neonatal mouse brains.

Fig. S3. Dose-dependent effects of ASO-22 on expression of $Na_V1.1$ in ICV-injected neonatal mouse brains.

Fig. S4. A control ASO promoted exon 35 exclusion of *Cep290* mRNA in neonatal mouse brain.

Fig. S5. Expression of *Scn1a* mRNA in mouse brains at different post-injection days.

Fig. S6. Expression of $Na_V1.1$ in mouse brains at different post-injection days.

Fig. S7. Numbers of $Scn1a^{+/-}$ mice that had 0, 1, or 2+ seizures after treatment.

Fig. S8. Validation of the two anti-$Na_V1.1$ antibodies.

Movie S1. Terminal seizure event in a DS mouse injected with 60 μg of ASO at P14.

Movie S2. Terminal seizure event in a DS mouse injected with 3 μl of PBS at P14.

Data file S1. Individual-level data for figures with *n* less than 20.

References (*29*, *30*)

View/request a protocol for this paper from *Bio-protocol*.

REFERENCES AND NOTES

1. C. Dravet, M. Bureau, B. B. Dalla, R. Guerrini, Severe myoclonic epilepsy in infancy (Dravet syndrome) 30 years later. *Epilepsia* **52** (suppl. 2), 1–2 (2011).
2. C. Dravet, M. Bureau, H. Oguni, Y. Fukuyama, O. Cokar, Severe myoclonic epilepsy in infancy: Dravet syndrome. *Adv. Neurol.* **95**, 71–102 (2005).
3. R. Guerrini, J. Aicardi, Epileptic encephalopathies with myoclonic seizures in infants and children (severe myoclonic epilepsy and myoclonic-astatic epilepsy). *J. Clin. Neurophysiol.* **20**, 449–461 (2003).
4. C. Dravet, The core Dravet syndrome phenotype. *Epilepsia* **52** (suppl. 2), 3–9 (2011).
5. M. S. Cooper, A. McIntosh, D. E. Crompton, J. M. McMahon, A. Schneider, K. Farrell, V. Ganesan, D. Gill, S. Kivity, T. Lerman-Sagie, A. McLellan, J. Pelekanos, V. Ramesh, L. Sadleir, E. Wirrell, I. E. Scheffer, Mortality in Dravet syndrome. *Epilepsy Res.* **128**, 43–47 (2016).
6. J. V. Skluzacek, K. P. Watts, O. Parsy, B. Wical, P. Camfield, Dravet syndrome and parent associations: The IDEA League experience with comorbid conditions, mortality, management, adaptation, and grief. *Epilepsia* **52** (suppl. 2), 95–101 (2011).
7. Y. W. Wu, J. Sullivan, S. S. McDaniel, M. H. Meisler, E. M. Walsh, S. X. Li, M. W. Kuzniewicz, Incidence of Dravet syndrome in a US population. *Pediatrics* **136**, e1310–e1315 (2015).
8. F. Brigo, P. Striano, G. Balagura, V. Belcastro, Emerging drugs for the treatment of Dravet syndrome. *Expert Opin. Emerg. Drugs* **23**, 261–269 (2018).
9. B. K. O'Connell, D. Gloss, O. Devinsky, Cannabinoids in treatment-resistant epilepsy: A review. *Epilepsy Behav.* **70**, 341–348 (2017).
10. M. L. Buck, H. P. Goodkin, Stiripentol: A novel antiseizure medication for the management of Dravet syndrome. *Ann. Pharmacother.* **53**, 1136–1144 (2019).
11. K. H. Lim, Z. Han, H. Y. Jeon, J. Kach, E. Jing, S. Weyn-Vanhentenryck, M. Downs, A. Corrionero, R. Oh, J. Scharner, A. Venkatesh, S. Ji, G. Liau, B. Ticho, H. Nash, I. Aznarez, Antisense oligonucleotide modulation of non-productive alternative splicing upregulates gene expression. *Nat. Commun.* **11**, 3501 (2020).
12. F. Lejeune, Nonsense-mediated mRNA decay at the crossroads of many cellular pathways. *BMB Rep.* **50**, 175–185 (2017).
13. A. M. Mistry, C. H. Thompson, A. R. Miller, C. G. Vanoye, A. L. George Jr., J. A. Kearney, Strain- and age-dependent hippocampal neuron sodium currents correlate with epilepsy severity in Dravet syndrome mice. *Neurobiol. Dis.* **65**, 1–11 (2014).
14. T. A. Zanardi, T.-W. Kim, L. Shen, D. Serota, C. Papagiannis, S.-Y. Park, Y. Kim, S. P. Henry, Chronic toxicity assessment of 2'-*O*-methoxyethyl antisense oligonucleotides in mice. *Nucleic Acid Ther.* **28**, 233–241 (2018).
15. N. A. Hawkins, N. J. Zachwieja, A. R. Miller, L. L. Anderson, J. A. Kearney, Fine mapping of a Dravet syndrome modifier locus on mouse chromosome 5 and candidate gene analysis by RNA-Seq. *PLOS Genet.* **12**, e1006398 (2016).
16. J. D. Calhoun, N. A. Hawkins, N. J. Zachwieja, J. A. Kearney, *Cacna1g* is a genetic modifier of epilepsy in a mouse model of Dravet syndrome. *Epilepsia* **58**, e111–e115 (2017).
17. E. C. Wirrell, L. Laux, E. Donner, N. Jette, K. Knupp, M. A. Meskis, I. Miller, J. Sullivan, M. Welborn, A. T. Berg, Optimizing the diagnosis and management of Dravet syndrome: Recommendations from a North American consensus panel. *Pediatr. Neurol.* **68**, 18–34.e3 (2017).
18. G. Colasante, G. Lignani, S. Brusco, C. Di Berardino, J. Carpenter, S. Giannelli, N. Valassina, S. Bido, R. Ricci, V. Castoldi, S. Marenna, T. Church, L. Massimino, G. Morabito, F. Benfenati, S. Schorge, L. Leocani, D. M. Kullmann, V. Broccoli, dCas9-based *Scn1a* gene activation restores inhibitory interneuron excitability and attenuates seizures in Dravet syndrome mice. *Mol. Ther.* **28**, 235–253 (2020).
19. T. Athanasopoulos, M. M. Munye, R. J. Yáñez-Muñoz, Nonintegrating gene therapy vectors. *Hematol. Oncol. Clin. North Am.* **31**, 753–770 (2017).
20. O. Khorkova, C. Wahlestedt, Oligonucleotide therapies for disorders of the nervous system. *Nat. Biotechnol.* **35**, 249–263 (2017).
21. D. R. Corey, Nusinersen, an antisense oligonucleotide drug for spinal muscular atrophy. *Nat. Neurosci.* **20**, 497–499 (2017).
22. G. L. Carvill, K. L. Engel, A. Ramamurthy, J. N. Cochran, J. Roovers, H. Stamberger, N. Lim, A. L. Schneider, G. Hollingsworth, D. H. Holder, B. M. Regan, J. Lawlor, L. Lagae, B. Ceulemans, E. M. Bebin, J. Nguyen; EuroEPINOMICS Rare Epilepsy Syndrome, Myoclonic-Astatic Epilepsy, and Dravet Working Group, G. S. Barsh, S. Weckhuysen, M. Meisler, S. F. Berkovic, P. De Jonghe, I. E. Scheffer, R. M. Myers, G. M. Cooper, H. C. Mefford, Aberrant inclusion of a poison exon causes Dravet syndrome and related *SCN1A*-associated genetic epilepsies. *Am. J. Hum. Genet.* **103**, 1022–1029 (2018).
23. C. Marini, I. E. Scheffer, R. Nabbout, A. Suls, P. De Jonghe, F. Zara, R. Guerrini, The genetics of Dravet syndrome. *Epilepsia* **52** (suppl. 2), 24–29 (2011).
24. S. Gataullina, O. Dulac, From genotype to phenotype in Dravet disease. *Seizure* **44**, 58–64 (2017).
25. H. Meng, H.-Q. Xu, L. Yu, G.-W. Lin, N. He, T. Su, Y.-W. Shi, B. Li, J. Wang, X.-R. Liu, B. Tang, Y.-S. Long, Y.-H. Yi, W.-P. Liao, The *SCN1A* mutation database: Updating information and analysis of the relationships among genotype, functional alteration, and phenotype. *Hum. Mutat.* **36**, 573–580 (2015).
26. L. R. F. Claes, L. Deprez, A. Suls, J. Baets, K. Smets, T. Van Dyck, T. Deconinck, A. Jordanova, P. De Jonghe, The *SCN1A* variant database: A novel research and diagnostic tool. *Hum. Mutat.* **30**, E904–E920 (2009).
27. L. G. Sadleir, E. I. Mountier, D. Gill, S. Davis, C. Joshi, C. DeVile, M. A. Kurian; DDD Study, S. Mandelstam, E. Wirrell, K. C. Nickels, H. R. Murali, G. Carvill, C. T. Myers, H. C. Mefford, I. E. Scheffer, Not all *SCN1A* epileptic encephalopathies are Dravet syndrome: Early profound Thr226Met phenotype. *Neurology* **89**, 1035–1042 (2017).

28. G. Berecki, A. Bryson, J. Terhag, S. Maljevic, E. V. Gazina, S. L. Hill, S. Petrou, *SCN1A* gain of function in early infantile encephalopathy. *Ann. Neurol.* **85**, 514–525 (2019).
29. Y. Hua, K. Sahashi, G. Hung, F. Rigo, M. A. Passini, C. F. Bennett, A. R. Krainer, Antisense correction of SMN2 splicing in the CNS rescues necrosis in a type III SMA mouse model. *Genes Dev.* **15**, 1634–1644 (2010).
30. X. Gérard, I. Perrault, A. Munnich, J. Kaplan, J.-M. Rozet, Intravitreal injection of splice-switching oligonucleotides to manipulate splicing in retinal cells. *Mol. Ther. Nucleic Acids* **4**, e250 (2015).

Acknowledgments: We thank J. Kearney from Northwestern University for providing the DS mice. We thank A. Goldman from Baylor College of Medicine, Center for SUDEP Research, for providing total RNA from the brain of a DS patient. We thank N. Zhao, Stoke Therapeutics Inc., for ASO evaluation and data analysis. **Funding:** This work was funded by a grant from Stoke Therapeutics Inc. (to L.L.I.). **Author contributions:** Z.H. designed and carried out the experiments, performed data analysis, and drafted the manuscript. C.C. carried out the experiments. A.C. designed the experiments, carried out data analysis, coordinated the research, and drafted the manuscript. S.J. carried out the experiments and performed data analysis. Q.L. carried out the LC-MS experiments and performed data analysis. C.A. carried out the experiments and analyzed the video monitoring data. C.L. carried out the experiments. S.C.L. carried out the EEG experiments. M. designed the experiments. I.A. designed the experiments and revised the manuscript. G.L. designed the experiments and drafted and revised the manuscript. L.L.I. designed the experiments and drafted and revised the manuscript. All authors read and approved the final manuscript. **Competing interests:** Z.H., A.C., S.J., Q.L., M., I.A., and G.L. are employees of Stoke Therapeutics Inc. C.C., C.A., C.L., S.C.L., and L.L.I. declare no competing interests. Z.H. and I.A. are inventors on patent/patent application # PCT/US2018/48031; WO/2019/040923 entitled "Antisense oligomers for the treatment of conditions and diseases" submitted by Stoke Therapeutics, Inc. that covers use of therapeutic agents to promote exclusion of the NMD exon from the NMD exon mRNA encoding NaV1.1. **Data and materials availability:** All the data are present in the manuscript or in the Supplementary Materials.

Submitted 24 September 2019
Resubmiited 27 March 2020
Accepted 3 June 2020
Published 26 August 2020
10.1126/scitranslmed.aaz6100

Citation: Z. Han, C. Chen, A. Christiansen, S. Ji, Q. Lin, C. Anumonwo, C. Liu, S. C. Leiser, I. Aznarez, G. Liau, L. L. Isom, Antisense oligonucleotides increase *Scn1a* expression and reduce seizures and SUDEP incidence in a mouse model of Dravet syndrome. *Sci. Transl. Med.* **12**, eaaz6100 (2020).